



AlCrVN coatings deposited by cathodic arc: Friction and wear properties evaluated using reciprocating sliding test

A. Delgado^a, O. Garcia-Zarco^b, J. Restrepo^c, S.E. Rodil^{b,*}

^a Posgrado en Ciencia e Ingeniería de Materiales, Universidad Nacional Autónoma de México, CDMX, México

^b Instituto de Investigaciones en Materiales, Universidad Nacional Autónoma de México, CDMX, México

^c SADOSA SA de CV, CDMX, México

ARTICLE INFO

Keywords:

Hard coatings

Linear reciprocating ball-on-flat

self-lubrication

Oxidation resistance

AlCrN coatings have long been used to endure the lifetime of cutting tools due to their high hardness and good mechanical qualities. Vanadium (V) additions to AlCrN coatings were studied for their mechanical and tribological properties against Al_2O_3 counterparts using the linear reciprocating sliding test. The AlCrN and AlCrVN coatings were deposited using cathodic multi-arc evaporation to steel substrates. We evaluated the effect of a high fraction of V into equimolar Al and Cr coatings, which is different from those reported in previous works. X-ray diffraction patterns and Raman spectroscopy demonstrated that the structure remained as the metastable face center cubic. Microindentation tests demonstrated that AlCrVN coating has a higher hardness than AlCrN coating, probably due to an improved microstructure and larger nitrogen incorporation. The wear resistance of the hard steel substrate was significantly increased using both hard coatings. However, no significant changes were observed in the coefficient of friction and wear rate. The results show that V addition significantly improved the mechanical and adhesive capabilities of the AlCrN coating without compromising the oxidation resistance at moderate temperatures (<500 °C).

1. Introduction

AlCrN thin coatings have been incorporated in the industry over the last few decades due to their high hardness, wear, and corrosion resistance [1–3]. Metastable face-centered cubic (fcc) AlCrN coatings exhibit exceptional oxidation resistance due to the production of protective

oxides Al_2O_3 and Cr_2O_3 that limit the O diffusion into the coating. However, like most of the hard coatings, the friction coefficient (CoF) tested against Al_2O_3 in the unidirectional ball-on-disk system is high 0.7 [4,5], which climbed to 1.0 at temperatures above 500 °C [5], a temperature range often encountered in cutting operations. Linear reciprocating sliding wear tests performed under dry conditions and against AISI52100 balls indicated a decrease in the CoF as the load increased, but the lowest value obtained in a treated substrate was above 0.5 [6], similar to other results [7]. Therefore, the search for addition of alloying elements such as Si, B, Zr, Y, and V has been investigated to improve the tribological film characteristics [8]. The addition of V into AlCrN coatings was deeply investigated by Franz et al. [5,9,10], who shows that under high bias conditions (−125 V), V enters the fcc crystalline phase forming an AlCrVN solid solution with hardness comparable to the AlCrN coating. Franz's works investigated a metallic V/(Al + Cr + V) ratio (V_{fraction}) from 0 to 0.28, keeping the Al content fixed while Cr was substituted by V [5,9], finding that at room temperature (RT), there was no effect of V in the CoF measured by a unidirectional sliding test against Al_2O_3 ball. Raising the test temperature to 500 °C, the CoF was initially increased, but at 700 °C, a significant reduction to 0.2 was obtained due to the formation of the lubricious V_2O_5 layer oxide that melts at 625 °C [9,11,12]. Later reports by Bobzin et al. [13] showed that the Cr rich CrAlVN coatings with a $V_{\text{fraction}} = 0.2$ deposited via a combination of magnetron sputter (MS) ion plating and high power pulse magnetron sputtering (HPPMS) also presented a reduction in the CoF from 0.6 at RT to 0.05 at 800 °C. Xu et al. [14] evaluated the oxidation resistance of

Abbreviations: AlCrVN, Aluminum-Chromium-Vanadium-nitride; CAE, Cathodic Arc Evaporation.

* Corresponding author.

E-mail address: srodil@unam.mx (S.E. Rodil).

<https://doi.org/10.1016/j.surfcoat.2022.128140>

Available online 25 January 2022

0257-8972/© 2022 Elsevier B.V. All rights reserved.

Table 1
Composition of AlCrVN coatings.

	Al/(Al + Cr + V)	V/(Al + Cr + V)
Franz [10]	0.71	0
	0.68	0.11
	0.67	0.16
	0.68	0.22
	0.68	0.28
Bobzin [13]	0.21	0.2
Xu [14]	0.48	0
	0.44	0.06
Tillman [15]	0.74	0
	0.67	0.07
	0.625	0.15
	0.57	0.22
	0.53	0.28

CrAlVN coatings with a small addition of V ($V_{\text{fraction}} = 0.06$), finding that the single fcc phase is retained and the hardness is increased from 30.8 GPa to 33.0 GPa due to a solid solution strengthening mechanism. However, similar to previous reports, the oxidation resistance is reduced due to the V addition. Tillman et al. [15] investigated the minimum amount of V required to improve the tribological response of AlCrN coatings deposited by magnetron sputtering. The Al/(Al + Cr + V) ratio was varied between 0.53 and 0.74, as the V_{fraction} increased from 0.07 to 0.28. The results indicate that it is important to have a large V fraction to observe a reduction in the CoF at high temperatures since otherwise, the oxide scale is not uniform and does not provide lubrication. The V_{fraction} investigated for these groups are summarized in Table 1, where it can be seen that V fractions above 0.28 have not been evaluated, probably to

avoid the hcp-AlN phase separation. However, the recent evidence that the maximum metastable solubility of Al in VAlN can be extended by metal-ion bombardment, open new insights to investigate the structure of V rich AlCrVN samples. Therefore, the aim in this work was to investigate the properties of V-rich AlCrVN deposited by the energetic arc deposition technique. Moreover, our interest was to determine if using a larger fraction of V, the flash temperatures during the sliding conditions could induce the formation of the lubricious vanadium oxide layer and the consequent reduction in friction.

Recently, Nguyen et al. [16] aiming to demonstrate the effectiveness of the AlCrVN for real applications, compared the tribological response of AlCrVN coatings deposited by multi-arc evaporation on untreated and plasma-nitrided surfaces of HS6-5-2 and H13 steels. No significant reduction in the CoF friction was observed, but the wear was 81–86% lower than for the uncoated steel. However, the coating composition is not reported. Different from previous works [5,13,17], Nguyen et al. [18] used the linear reciprocating test to evaluate the wear, which according to Klaffke et al. [19], allows more accurate quantification of the wear for high resistant coatings since the determination of the volumetric wear is more precise due to the shorter wear length than in continuous pin-on-disk sliding. The cutting performance of arc deposited AlCrXN coatings (X = V and Mo) was assessed by [20]. The AlCrXN coatings preserved the fcc solid solution after the addition of V or Mo and an increment in the hardness, but the exact composition was not reported. Wang et al. [21] evaluated the inclusion of V into AlCrSiN coatings deposited by a hybrid ion plating-sputtering system, finding that the fcc-Cr(Al, V)N solid solution could be retained for high percentages of V (20 at.%), the deposition rate was increased, and the

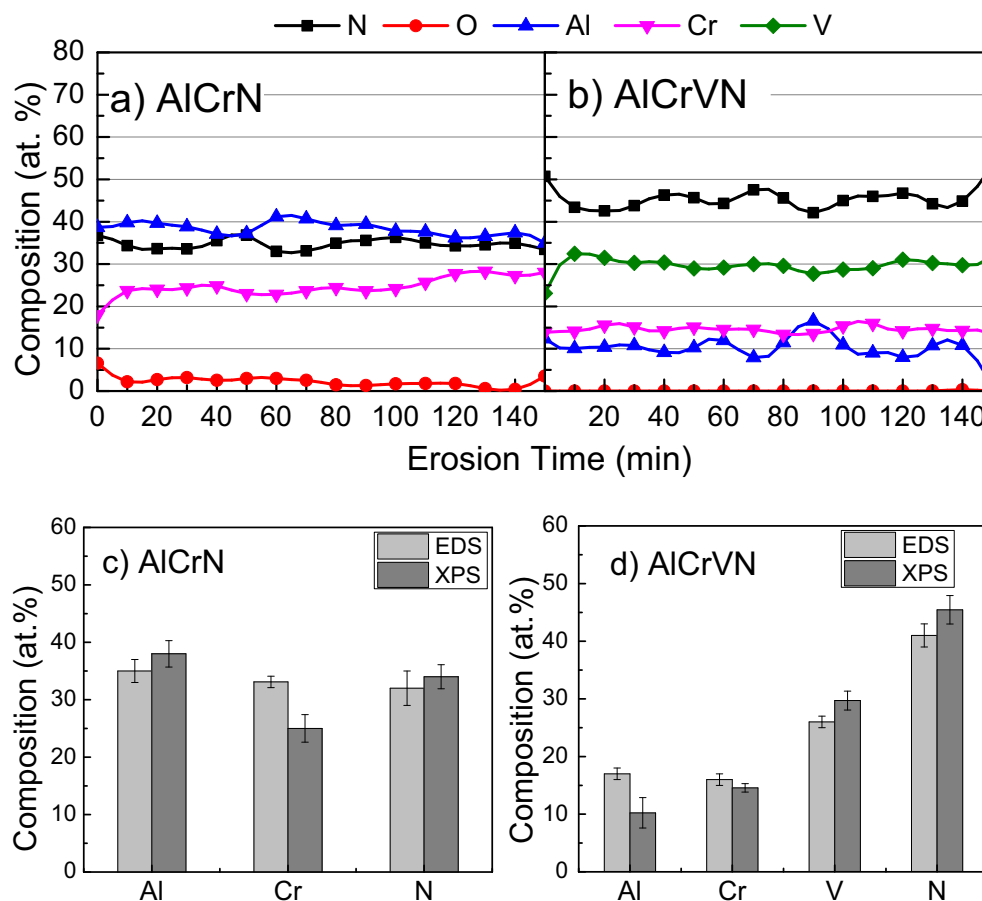


Fig. 1. Composition of the AlCrN and AlCrVN coatings. Depth profile obtained by X-ray photoelectron spectroscopy to a maximum depth of 450 nm for a) AlCrN and b) AlCrVN. Comparison of the composition obtained by XPS and EDX for c) AlCrN and d) AlCrVN. Small variations are due to the different volumes analyzed by each technique.

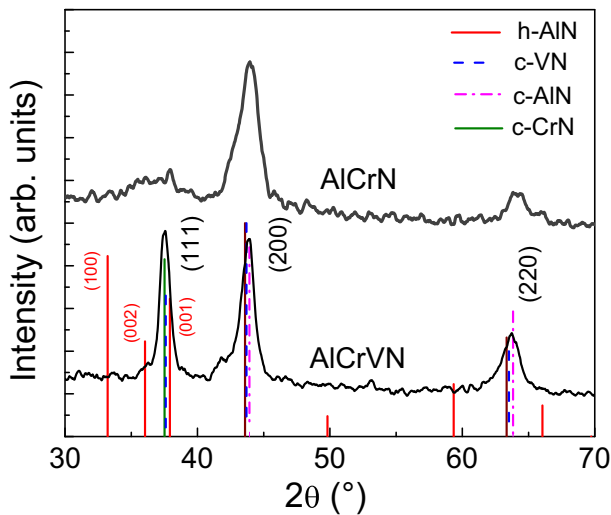


Fig. 2. Representative grazing incidence XRD patterns of both coatings deposited on D2 substrates.

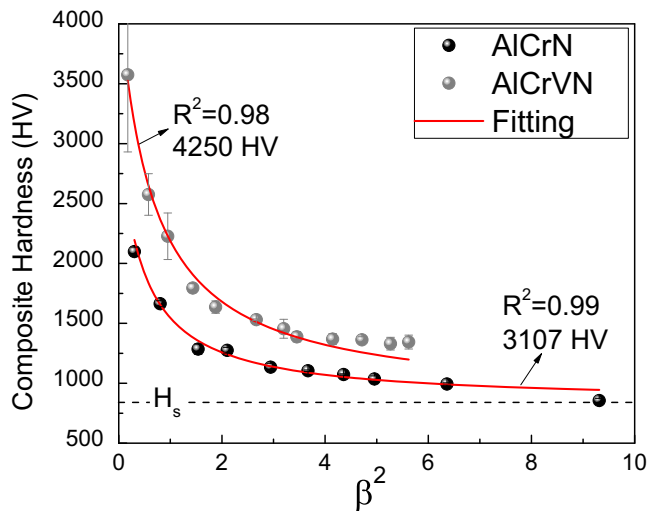


Fig. 3. Fittings of the Vickers composite hardness to obtain the film hardness.

hardness shows a maximum when V was 13.5 at.%. No differences in friction were observed at room temperature, but a significant decrease from 0.9 to 0.21 was observed at 800 °C at the highest V fraction. Nevertheless, the wear rates were increased.

In this work, we evaluate the mechanical and room temperature tribological properties of AlCrVN coatings with an Al/(Al + Cr + V) ratio of 0.51 and V_{fraction} of 0.44 deposited using an industrial cathodic arc system. The linear reciprocating system was selected and used against the hard Al_2O_3 to better identify the properties of the coating.

2. Experimental details

2.1. Coating's deposition

The coatings were deposited using an industrial cathodic arc evaporation (CAE) system with 12 targets distributed symmetrically around a cylindrical chamber [22]. Only one-third of the cathodes were used, corresponding to the lower section of the system, as shown in Fig. S1. For the AlCrN coatings, four AlCr (66/33 at.%) targets were used, and for the AlCrVN, two targets were substituted by V targets (99.5 at.%); the target-substrate distance is 135 mm. The coatings were

simultaneously deposited on mirror polished metallic substrates, placed in an 80 mm rotating orbital substrate holder (50 s/turn): stainless steel (SS), high-speed M2, and D2 steels. The vacuum chamber was evacuated by a diffusion pump to a base pressure of 8.0×10^{-3} Pa, and coatings were done at 3.5 Pa of pure N_2 atmosphere. The substrates were pre-heated for 90 min at 450 °C and cleaned by plasma etching with Ar ions at 750 V. The current applied to the AlCr targets was −85 A and to the V targets −50 A. A substrate bias of −125 V was applied for both coatings.

2.2. Coating's properties

The structure was evaluated by X-ray diffraction (XRD) and Raman (M2 and D2 substrates), while the composition was obtained using X-ray photoelectron spectroscopy (XPS) for coatings deposited on SS. X-ray diffraction characterization was done using a Rigaku Ultima IV diffractometer with $\text{Cu K}\alpha$ radiation, in grazing incidence mode, with an incidence angle of 0.5° , acquisition step 0.02° and scanning speed of $0.5^\circ \text{ min}^{-1}$. The identification of the phase was verified through micro-Raman spectroscopy using a RSpectre 532 spectrometer with a wavelength laser of 532 nm, power density of 3876 W cm^{-2} , a lens with a magnification of $60\times$. Spectra were recorded at different zones of the coating to confirm homogeneity, and each one was the average of 60 acquisitions with an exposure time of 1 s.

The chemical composition of the coatings was determined by X-ray photoelectron spectroscopy (XPS) using a Physical Electronics®, Scanning XPS microprobe PHI 5000 VersaProbe II spectrometer, with an MCD detector and radiation source of Al $\text{K}\alpha$ ($h\nu = 1486.6 \text{ eV}$). Pass energy of 117.4 and 11.75 eV were used for the acquisition of the survey and high-resolution spectra, respectively. Depth profile spectra were obtained bombarding the surface with Ar ions 3 kV, 3 μA , in a $3 \times 3 \text{ mm}$ area for 5 min, during 30 cycles to reach a total of 150 min of erosion. The equivalent thickness analyzed was approximately 450 nm obtained using the same erosion parameters in thinner coatings of the same composition.

The composition of the coating and the wear tracks were evaluated by energy dispersive X-ray fluorescence (EDX) in scanning electron microscopy (SEM), taking at least five different zones. Surface images of the samples were obtained by a field-emission gun scanning electron microscopy (FESEM) JEOL7600F.

The topography of the samples was measured using a Zygo Nex-view™ optical profilometer, and the images were analyzed through Mx™ version 6.4.0.21 software.

The coatings produced by this unfiltered cathodic arc system have a distinct surface roughness attributed to the generation of macroparticles within the cathode spot and their incorporation into the growing film. Thus, hardness determination using nanoindentation becomes difficult. Therefore, we use the Korsunsky composite hardness model to estimate variations in the mechanical properties due to the incorporation of V [23,24]. According to the model, the coatings' hardness (H_f) is calculated using the Korsunsky equation [23]

$$H_c = H_s + \frac{(H_f - H_s)}{(1 + k\beta^2)} \quad (1)$$

where H_s is the substrate's hardness, $\beta = d / 7t$, d is the average diagonal, t the film thickness. H_f and k are the only two parameters determined by the fitting of the H_c versus β^2 curve (or different load values). As described by Korsunsky et al. [23], the quality of the fit relies on obtaining experimental hardness data over a wide range of penetration values (β). Therefore, H_c values were obtained employing loads between 2 and 24 N, every 2 N. At least five measurements were conducted for each load applied using a Nanovea PB 1000 system. The substrate hardness, H_s , was previously measured and used as a fixed parameter.

The adhesion of the coatings was evaluated by the scratch test using the nanovea PB 1000 system. For these tests, the Rockwell diamond

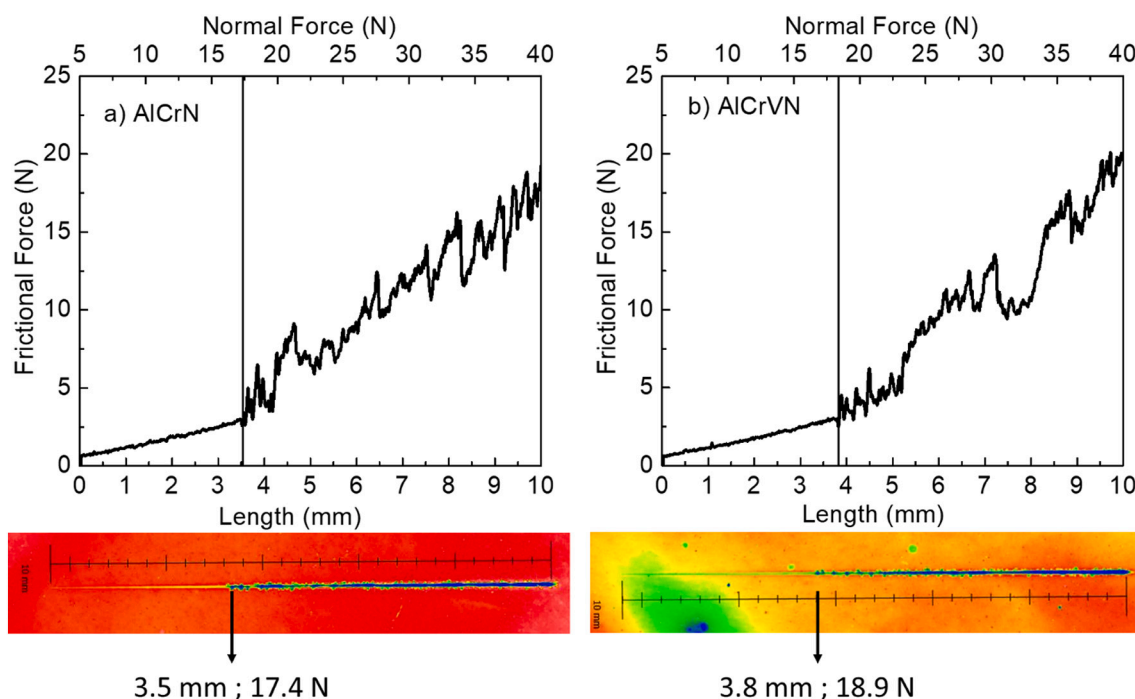


Fig. 4. Scratch test to determine the coating-substrate adhesion. a) AlCrN, and b) AlCrVN. The critical loads defined by the analysis of both the CoF plots and the images are compared.

indenter with a rounded tip in radius of 200 μm was used. A sliding speed of 10 N/min, and a moving distance of 10 mm were used. The normal load was linearly increased from 5 to 40 N. The critical loads were determined using the signal of the friction coefficient and analysis of the optical profilometer.

The friction-wear quality of the coatings was assessed using the linearly reciprocating ball-on-flat method. Friction-wear experiments were conducted at 18–21 $^{\circ}\text{C}$ and 50% relative humidity using the nanovea PB 1000 system tester without lubrication. The opposing material was Al_2O_3 balls with a diameter of 6.0 mm and an average roughness of 2 μm . Three test loads were evaluated up to 200 cycles: 5, 10, and 20 N. Meanwhile, a longer test was run at 5000 cycles and 25 N and used to evaluate the wear volume (W_V) and rate (k). The wear volume was estimated using non-contact 3D optical surface metrology as described by Ayerdi et al. [25].

In order to evaluate the oxidation resistance of the coating at moderate temperatures, the coatings were annealed in air at 460 $^{\circ}\text{C}$ (the maximum temperature that the D2 steel can withstand before changing its mechanical properties) for 1 h. Then, the composition was analyzed by depth-profile XPS as described above.

3. Results and discussion

3.1. Composition

The surface composition of the as-deposited AlCrN and AlCrVN coatings deposited on the SS substrates was obtained by XPS as a function of the erosion time and is shown in Fig. 1. The SS substrates were used since D2 and M2 are magnetic and interfere with the emitted photoelectrons.

The coating's composition was measured by XPS up to an approximate depth of 450 nm. The results presented in Fig. 1a and b indicated a relatively uniform composition, with some oscillation in the Al content and very few O contents inside the coatings (it goes to zero for the AlCrVN). The high-resolution spectra as a function of depth (Fig. S2) show that the bonding characteristics of the metallic elements are stable in-depth, indicating mainly a nitride environment. Fig. 1c and d shows

the comparison between the composition obtained by EDX (samples deposited on the D2 substrate) and the average value of the XPS data, where a good agreement between both measurements can be observed. According to the EDX data, the Al/Cr ratio of the coatings is 1.0 for AlCrN and 1.1 for AlCrVN, values which are reduced in comparison to the target ratio ($\text{Al/Cr} = 2$). Small Al deficiency was also observed by Franz et al. [5] for the arc deposited AlCrN coatings [5]. It is probably explained by displacement of the lightest Al element when Cr and/or V atoms impinge on the substrate. For our AlCrVN coating, the predominant metallic element is V. Moreover, the nitrogen incorporation is higher in the AlCrVN coating than without V. An effect explained because V has a stronger binding capacity with N than both Al and Cr [14], leading to an easier bond formation of V–N bonds in comparison to Al–N or Cr–N.

The thickness of the coatings was measured by a homemade ball cratering system. Optical micrographs of the abraded area using a stainless-steel ball of 25 mm of diameter are shown in Fig. S3. The thickness was estimated by comparing the relative diameters of the exposed surface layers to the known ball diameter. It was slightly larger for the AlCrVN coating (3.85 μm vs. 3.38 μm), although the current applied to the V target was lower than for the AlCr targets, which is an indicator of a large erosion rate for the V. This is in contrast with the lower sputter yield of V in comparison to Al and Cr when sputtering is used for the deposition. A similar increase in the deposition rate was observed by Wang et al. [21] for the AlCrVSiN samples as the V content was increased.

3.2. Structure

Although some variations were obtained in the Al and Cr contents because of V addition, the $\text{Al}/(\text{Al} + \text{Cr})$ ratio remained below 0.7 for both samples, avoiding the threshold of the hexagonal wurtzite transformation content [9]. The XRD data (Fig. 2) suggest that both coatings presented mainly the fcc-crystal structure as confirmed by Raman spectroscopy [26] (Fig. S4). The dominant diffraction peaks correspond to the (111), (200), and (220) orientation and are situated between the position for fcc-CrN and fcc-AlN. The AlCrVN presents the two distinct

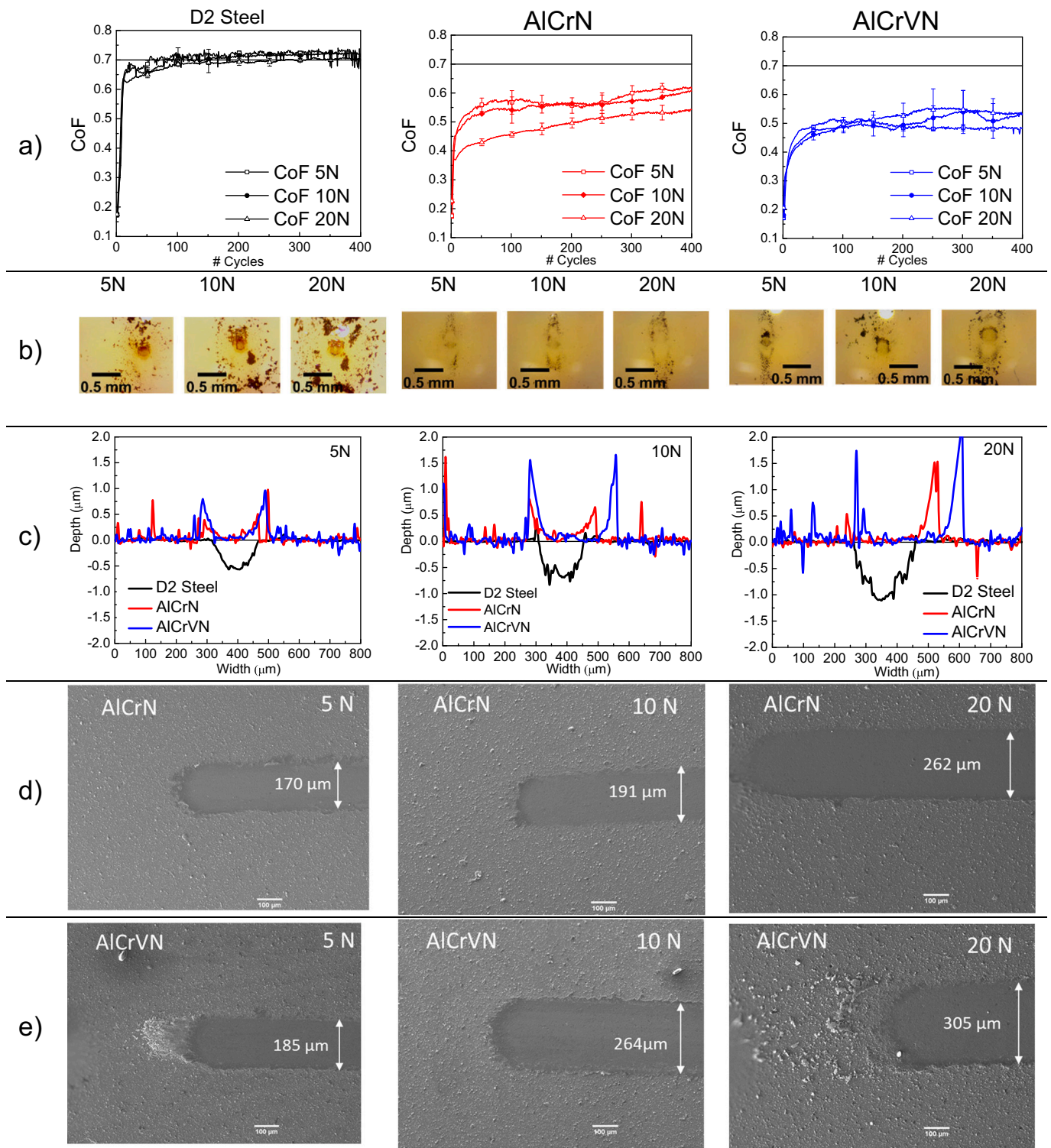


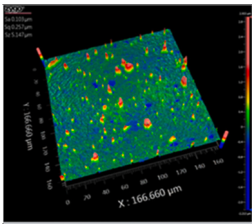
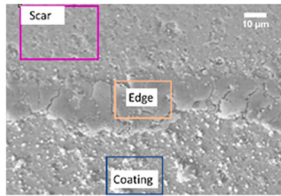
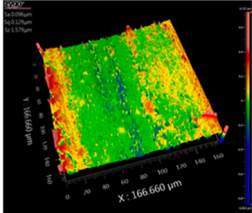
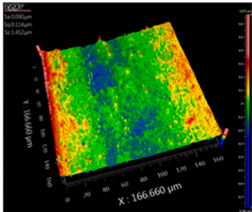
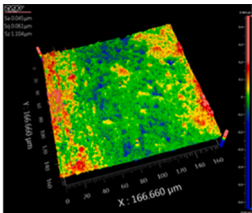
Fig. 5. Results of the linear reciprocating test. a) Plots of the coefficient of friction (CoF) as a function of the cycles and the normal load for the D2 substrate and the AlCrN and AlCrVN coatings. b) Optical microscopy images of the ball scar after testing the samples at each specific normal load. c) Representative profile obtained from the wear track using the optical profilometer for the D2 substrate and the coatings. Representative SEM images of the wear scar in the AlCrN d) and the AlCrVN e) coating.

(111) and (200) diffraction peaks of similar height; meanwhile, the AlCrN presents a lower (111) signal. This change in the preferred orientation as the V substitutes Al/Cr atoms in the structure might be associated with a process to compensate the increase in strain energy due to the lattice distortion created by V addition. The AlCrN has a preferred orientation in the (200) plane, which corresponds to the

minimum surface energy plane, an effect normally observed during film growth. To reduce the strain energy created by V addition, the preferred orientation changes towards the plane of highest surface energy [27]. The increase in peak intensity for the AlCrVN coating might be due to the larger nitrogen content. From this macroscopic analysis, possible segregation of VN cannot be discerned since the fcc diffraction signals

Table 2

Summary of the roughness and composition analysis performed for the AlCrN coating at the wear track for the three normal loads used in the linear reciprocating test. Sa is the average roughness, and Sz is the highest peak. The composition was obtained outside the wear track (coating), at the edge of the wear track, and inside the wear track (scar). The presented values are the average of five different EDX measurements.

Coating	Roughness (μm)	Image				
	Sa = 0.1 ± 0.01					
	Sz = 4.67 ± 0.41					
Wear scar			Composition (at.%)			
5 N	Sa = 0.08 ± 0.01		Load	Al	Cr	N
	Sz = 1.37 ± 0.08		Coating	34 ± 1	34 ± 1	32 ± 2
			Scar	34 ± 2	32 ± 2	34 ± 4
			Edge	41 ± 1	37 ± 1	22 ± 0.2
10 N	Sa = 0.07 ± 0.01		Composition (at.%)			
	Sz = 1.33 ± 0.23			Al	Cr	N
			Coating	35 ± 2	33 ± 1	32 ± 3
			Scar	37 ± 2	34 ± 1	30 ± 3
			Edge	60 ± 2	40 ± 2	0
20 N	Sa = 0.04 ± 0.01		Composition (at.%)			
	Sz = 1.12 ± 0.28			Al	Cr	N
			Coating	34 ± 1	33 ± 1	33 ± 2
			Scar	36 ± 2	33 ± 1	31 ± 3
			Edge	38 ± 3	35 ± 2	27 ± 5

for the three nitrides are very close in position. There is a small shoulder in both samples that could be associated with the (002) plane of the wurtzite hexagonal AlN, but the most intense (100) peak of the hcp-AlN phase is not revealed.

3.3. Hardness

Fig. 3 shows an example of the fitting of the composite hardness versus the β value following Eq. (1). The substrate hardness was fixed to the value measured for the substrate (844 for the M2 steel).

It can be seen that good fittings can be obtained for both samples with correlation values close to unity. The Vickers hardness obtained from the Korsunsky equation is 3107 ± 197 HV for AlCrN and 4250 ± 162 HV for AlCrVN. The saturation of the composite hardness at low penetration depths (low β values) is not observed, so the calculated hardness might be underestimated since they are slightly larger than those previously reported [9,13,15,28]. However, the measurements were repeated three times using any of the hard steel substrates (M2 or D2), and in all cases, we observed an increase in the hardness with the addition of V, which is similar to the reported trend observed by Franz et al. for AlCrVN samples retaining the fcc-crystal structure [9]. Regardless of the absolute hardness values, the shallower penetration depths (lower β values) and larger composite hardness measured for the AlCrVN coatings indicates that the incorporation of V enhanced the mechanical resistance to penetration of the coatings.

3.4. Adhesion strength

One important property that determines the tribological performance of the coatings is the adhesion strength. Fig. 4 shows the variation of the frictional force as a function of the distance and normal force, together with the optical profilometry image of the scratch. For the AlCrN coating, the Lc1 occurs at 17.4 N; the film cracks, suffering cluster delamination around the track. For the AlCrVN, the Lc1 is similar at about 18.9 N. Complete failure of both coating is expected above 27 N, and this value determines the maximum load at which the friction test should be performed.

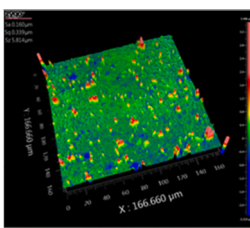
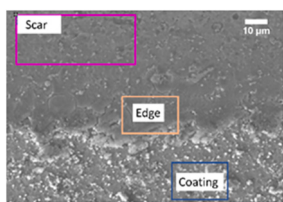
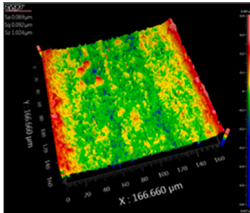
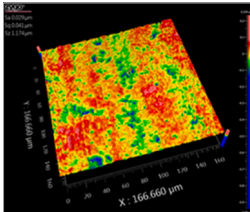
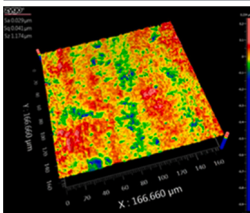
3.5. Friction-wear properties

The friction curves obtained from the linear reciprocating tests performed at 5, 10, and 20 N of load during 400 cycles (equivalent to a total distance of 8 m) are presented in Fig. 5, including also the D2 substrate as a reference and the micrographs taken from the counterface. The CoF plot (Fig. 5a) is the average from three different measurements for each condition.

For the D2 steel, the CoF is independent of the normal load presenting a steady-state value of 0.7. However, the wear volume increased from 4×10^5 to $12 \times 10^5 \mu\text{m}^3$ as the load increased from 5 to 20 N. The optical micrographs of the ball counterface show a maximum amount of attached debris in comparison to the coatings.

Table 3

Summary of the roughness and composition analysis performed for the AlCrVN coating around the wear track for the three normal loads used in the linear reciprocating test. Sa is the average roughness, and Sz is the highest peak. The composition was obtained outside the wear track (coating), at the edge of the wear track, and inside the wear track (scar). The presented values are the average of five different EDX measurements.

Coating	Roughness (μm)	Image					
	Sa = 0.16 ± 0.01						
	Sz = 6.05 ± 0.67						
Wear scar							
5 N	Sa = 0.076 ± 0.01		Composition (at.%)				
	Sz = 1.18 ± 0.09		Coating	Al	Cr	V	N
			Scar	17 ± 1	15 ± 1	25 ± 1	43 ± 3
			Edge	18 ± 1	15 ± 1	26 ± 1	41 ± 2
				21 ± 1	16 ± 1	26 ± 1	37 ± 2
10 N							
	Sa = 0.04 ± 0.01		Composition (at.%)				
	Sz = 1.14 ± 0.15		Coating	Al	Cr	V	N
			Scar	17 ± 1	16 ± 1	26 ± 1	41 ± 2
			Edge	17 ± 0.4	15 ± 1	25 ± 1	42 ± 1
				19	14 ± 0.2	25 ± 1	41 ± 1
20 N							
	Sa = 0.04 ± 0.01		Composition (at.%)				
	Sz = 1.02 ± 0.12		Coating	Al	Cr	V	N
			Scar	16 ± 1	15 ± 0.4	27 ± 1	42 ± 2
			Edge	17 ± 1	14 ± 1	25 ± 1	44 ± 2
				Not measured			

For both coatings, no visible wear could be observed, but an accumulation of material at the border of the wear track (Fig. 5c). The friction coefficients are slightly lower than between the D2-Al₂O₃ pair. AlCrN shows steady-state values decreasing with the normal load from 0.56 ± 0.04 at 5 N to 0.48 ± 0.04 at 20 N. Meanwhile, no variation in the CoF vs. load is observed for the AlCrVN sample, which reaches on average about 0.5 ± 0.04 at the three loads. There is a significant change in the mark left at the ball counterface, which is more elliptical and with debris distributed symmetrically in contrast to the steel, where a random distribution was observed.

The depth profiles and SEM images (Fig. 5d and e) show that the width of the wear track increases with the load for both coatings, and it is always larger in the AlCrVN coating, suggesting larger wear. However, as observed in the depth profiles, no significant volume loss was observed for both coatings at the tested conditions.

Analysis of the wear track shows that the main effect of the reciprocating test at these loads was a smoothing of the worn surface, i. e., a polishing wear mechanism, as can be observed in Tables 2 and 3 for AlCrN and AlCrVN, respectively. The as-deposited coatings exhibited larger average roughness (Sa) and maximum height peaks (Sz) than the worn surface. Such roughness is mainly associated with the macroparticles produced during the unfiltered arc deposition process. Both roughness parameters (Sa and Sz) decreased with the applied load but seemed to reach a minimum value. The wear track is distinguished by the accumulation of wear debris at both sides, that as can be seen in the

SEM images, show a sheet/flake-like morphology with clear cracks indicating delamination.

The elemental composition was investigated in three sections: inside, outside, and at the edges of the wear track. The data in Tables 2 and 3 shows that the composition was nearly the same inside and outside, which also correspond to the values reported in Fig. 1 for the coatings. However, significant variations in composition were detected at the edges where a reduced nitrogen content was observed. There is either a loss of nitrogen, or the material at the edges corresponds to the displaced and plastically deformed macroparticles, which are mainly metallic.

Tables 2 and 3 show that the average surface roughness of the as-deposited coatings is slightly larger for the AlCrVN coating than AlCrN but are in a similar range as values reported by [18,28] for arc deposited samples. In both cases, the surface is filled with macroparticles emitted during the deposition. These macroparticles are smeared out and suffer plastic deformation during the reciprocating friction test, probably accumulating at the edges. Analysis using Raman spectroscopy to identify the structure variations in each zone is presented in Figs. S4 and S5. There is no significant variation for the AlCrN coating that presents mainly the characteristic signal of the fcc structure [26,29] in all zones. However, for the AlCrVN coating, new broad bands around $900\text{--}950\text{ cm}^{-1}$ are observed in the wear track and edges. The spectra are not well defined to give a perfect identification, but the signals could be due to chromium oxides, aluminum oxides [8], AlVO₄, or vanadium oxide phases [12,30]. These oxides could be formed due to the very high flash

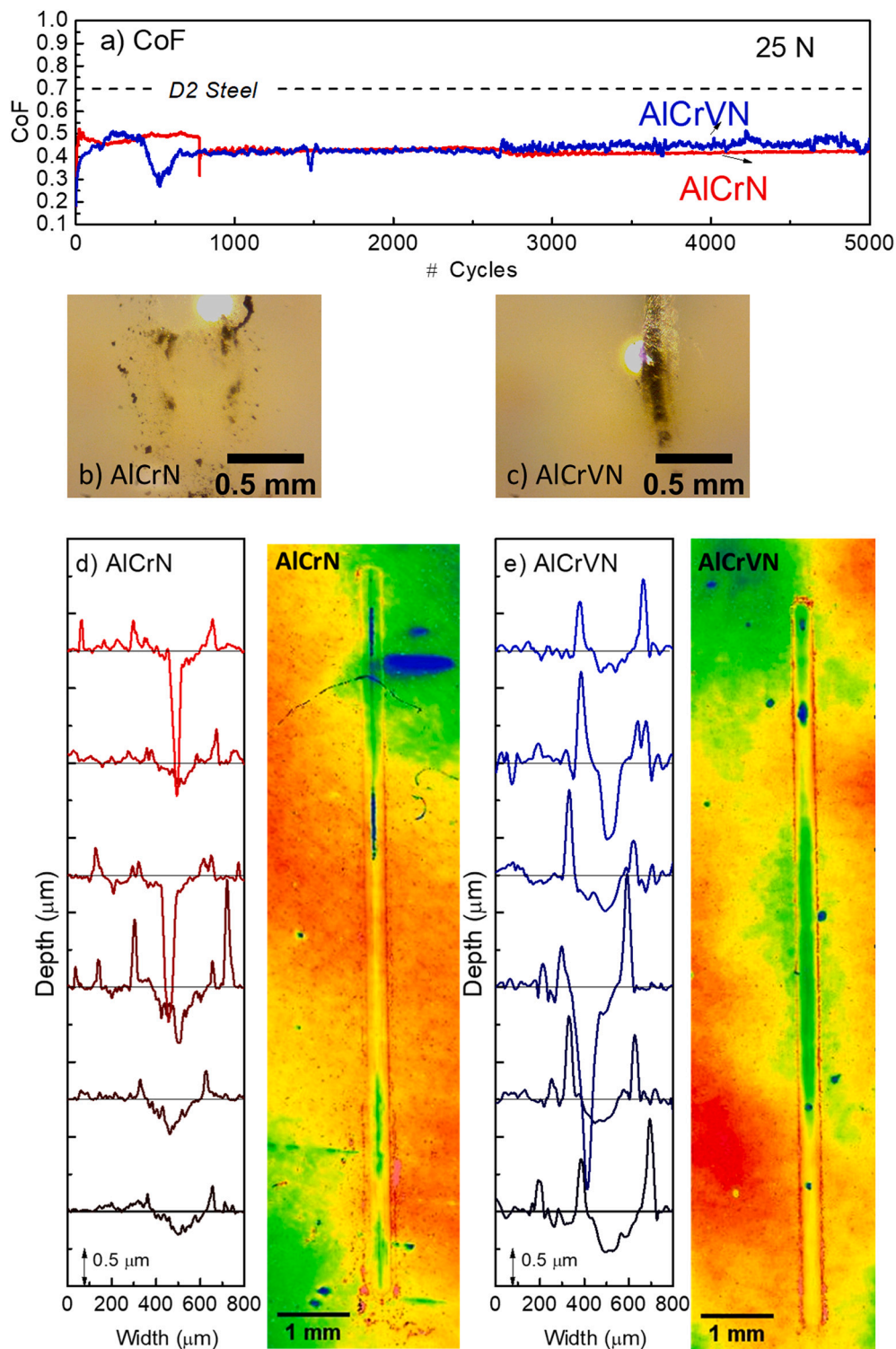


Fig. 6. Results of the 5000 cycles linear reciprocating test. a) Plots of the coefficient of friction (CoF) vs. cycles for the AlCrN and AlCrVN coatings. b), c) Optical images of the Al₂O₃ ball against AlCrN and AlCrVN. d), e) Optical profile of the wear track, including the depth profiles taken in different zones. Blue color corresponds to the deepest area and red to the highest.

temperatures attained at the coatings' asperities during the RT reciprocating tests [31]. These results indicated that despite the larger hardness and similar CoF, the AlCrVN coatings presented a wider wear track, which is probably due to the initiation of abrasive wear induced by the hard Al or Cr oxide layers [8] or it is a consequence of the larger roughness, particularly the larger size of the defects (Sz).

Nevertheless, both coatings were highly resistant, and no wear

volume could be measured up to the 400 cycles and 20 N of load. Therefore, to have a realistic estimate of the differences in wear between the coatings, another experiment using 25 N and 5000 cycles (equivalent to 100 m) was performed. Fig. 6a shows the CoF variation as a function of the cycles.

The CoF looks unstable for the initial 1000 cycles, and after, it is slightly reduced and remains stable for both coatings up to the end of the

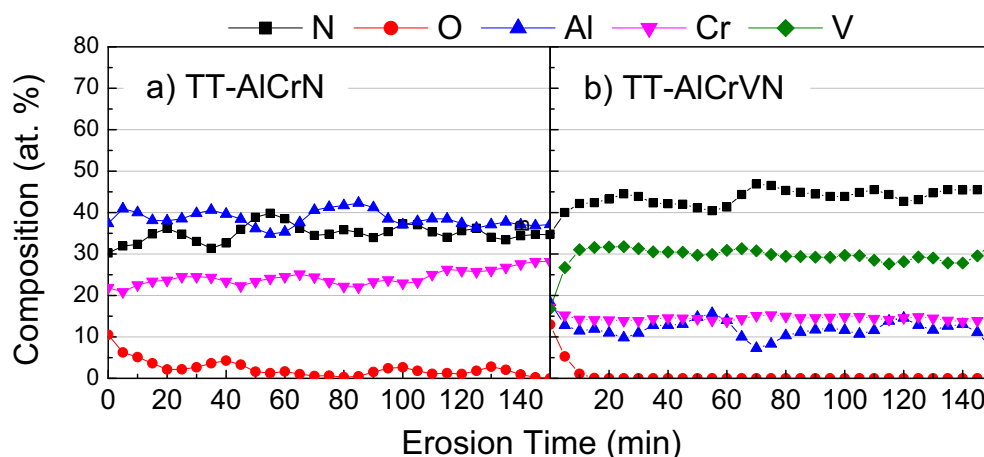


Fig. 7. Depth profile obtained by X-ray photoelectron spectroscopy to a maximum depth of 450 nm for the 460 °C annealed coatings a) AlCrN and b) AlCrVN.

test. The steady-state value is about 0.43 but larger and noisy for the AlCrVN coating, probably due to the larger roughness. Fig. 6d and e shows the complete wear track where the non-homogeneity of the depth is observed by the contrast in color and in the randomly taken profiles at different zones. The deepest (blue) wear depths correspond to localized damage areas observed in both samples, which might be related to the remotion of large macroparticles causing localized damage and deep worn areas. The non-homogeneity of the wear track depth makes unreliable the determination of the wear volume using only a few selected profiles. Therefore the total worn volume was computed using non-contact 3D optical surface metrology following the methodology described by Ayerdi et al. [25]. The results indicate that the wear loss volume was very similar, achieving $7.2 \times 10^{-4} \text{ mm}^3$ for AlCrN and $6.7 \times 10^{-4} \text{ mm}^3$ for AlCrVN. Considering the 25 cycles, 10 mm length, and the 25 N normal force, the wear rates, k , are both in the $10^{-7} \text{ mm}^3 \text{ N}^{-1} \text{ m}^{-1}$ range (5.76×10^{-7} and $5.36 \times 10^{-7} \text{ mm}^3 \text{ N}^{-1} \text{ m}^{-1}$ for AlCrN and AlCrVN, respectively), values which are no significantly different.

3.6. Oxidation resistance

Finally, to evaluate the effect of the V concentration on the oxidation resistance of the AlCrN coatings, the samples deposited on SS and D2 substrates were annealed in air at 460 °C for 1 h. The depth profiles obtained using XPS under the same conditions as the profile in Fig. 1 are presented in Fig. 7. It can be observed that at this annealing temperature, oxygen penetrates only a few layers into the coating, in which a slight increase in the signal from Al and Cr is also observed. The surface oxide is composed of Al and Cr oxides, and there is no migration of V towards the outer surface. This agrees with the annealing experiments presented previously by Franz et al. [11] and Bobzin et al. [13], providing an explanation to why the CoF is not reduced by the addition of V.

3.7. Discussion

The aim of this work was to determine the effect of a high fraction of V addition into AlCrN coatings deposited by CAE. Consequently, we used conditions for the synthesis which are different from those previously reported in which composite AlCrV or AlCr/CrV targets were used. In our case, the coatings were obtained from a co-deposition of AlCr and pure V targets since we were interested in increasing the content of vanadium above the reported values. As shown in Table 1, previous works evaluated a maximum V metallic fraction of 0.28, while we used 0.44. Based on the recent results that indicated that the solubility limit of the fcc AlN phases into the CrN/VN could be extended using energetic conditions, the samples were deposited by the CAE method using a high

substrate bias (−125 V). The interest in using V is to reduce the CoF, but it has been shown that it only works at temperatures above 600 °C where the V-rich oxide scales control the friction. Whether a larger V_{fraction} could benefit the sliding or not, as it has been observed in TiSiVN coatings [32,33], has not been previously reported. Our results indicated that AlCrVN coatings with V content as high as ~30 at.% could be produced, and the coatings presented a solid solution similar to the cubic CrN pattern, but this high V_{fraction} did not induce a significant reduction in the coefficient of friction or the wear volume, although the coating's hardness was increased. The linear reciprocating test using 6 mm Al_2O_3 balls at normal loads of 5, 10, and 20 N was characterized by a polishing wear mechanism since the average roughness in the wear track was reduced. This polishing was probably controlled by the growth defects (microdroplets) that were plastically deformed and accumulated at the borders of the wear track, as confirmed by the localized EDX analysis. The steady-state CoF was slightly lower than those reported by Nguyen et al. [16], who also used reciprocating sliding tests (10 N and 6.35 mm WC-balls). Larger load (25 N) and cycles were required to observe measurable wear in both coatings. In this case, a non-homogenous wear track was obtained, where again the defects have a strong negative impact causing localized abrasive wear with spalling of the coatings in some areas. Nevertheless, the wear rates are in the $10^{-7} \text{ mm}^3 \text{ N}^{-1} \text{ m}^{-1}$ range, meaning a large resistance, but without a significant contribution from the V addition. One possible explanation is that the large oxidation resistance of the AlCrN coatings impedes the migration of V to the surface at the temperatures reached during the sliding experiments. This was confirmed by analyzing the depth profiles of the coatings after annealing at 460 °C, where no formation of vanadium oxides was observed.

4. Conclusions

V-rich AlCrVN coatings were deposited using an industrial cathodic arc evaporation system using two AlCr targets and two V targets. The AlCrVN coatings presented the fcc-crystal structure with a random orientation, V addition led to an increment in the hardness by a 1.4 factor, and the oxidation resistance was retained for annealing treatments up to 460 °C. However, the tribological evaluation performed using the linear reciprocating test against 6 mm Al_2O_3 balls indicated that the addition of V into the AlCrN coating does not improve the tribological response. No visible wear was observed after testing at 5, 10, and 20 N for 100 cycles for both coatings. The room temperature CoF for a long test of 5000 cycles at 25 N reached very similar values of 0.43 and reduced wear rates ($10^{-7} \text{ mm}^3 \text{ N}^{-1} \text{ m}^{-1}$) for both coatings. No significant advantage of adding a high fraction of V in the tribological response of AlCrN coatings could be identified, although the XRD confirmed the

formation of a cubic solid solution.

Declaration of competing interest

The authors declare that they have no known competing financial interests or personal relationships that could have appeared to influence the work reported in this paper.

Acknowledgements

Authors thank the technical assistance of O. Novelo, L. Huerta, L. Bazan, A. Tejada, and C. Ramos. Financial support was provided by the SECTEI under grant number 201/2019.

Appendix A. Supplementary data

Supplementary data to this article can be found online at <https://doi.org/10.1016/j.surfcoat.2022.128140>.

References

- [1] J.L. Mo, M.H. Zhu, B. Lei, Y.X. Leng, N. Huang, *Wear* 263 (2007) 1423–1429.
- [2] R.D. Patel, S.N. Bhavsar, *Mater. Today Proc.* 22 (2020) 2647–2656.
- [3] J.L. Mo, M.H. Zhu, A. Leyland, A. Matthews, *Surf. Coat. Technol.* 215 (2013) 170–177.
- [4] M. Antonov, H. Afshari, J. Baronins, E. Adoberg, T. Raadik, I. Hussainova, *Tribol. Int.* 118 (2018) 500–514.
- [5] R. Franz, J. Neidhardt, B. Sartory, R. Kaindl, R. Tessadri, P. Polcik, V.H. Derflinger, C. Mitterer, *Tribol. Lett.* 23 (2006) 101–107.
- [6] I.S. Cho, A. Amanov, J.D. Kim, *Tribol. Int.* 81 (2015) 61–72.
- [7] R. Lan, C. Wang, Z. Ma, G. Lu, P. Wang, J. Han, *Mater. Res. Express* 6 (2019).
- [8] J.C. Sánchez-López, A. Contreras, S. Domínguez-Meister, A. García-Luis, M. Brizuela, *Thin Solid Films* 550 (2014) 413–420.
- [9] R. Franz, J. Neidhardt, R. Kaindl, B. Sartory, R. Tessadri, M. Lechthaler, P. Polcik, C. Mitterer, *Surf. Coat. Technol.* 203 (2009) 1101–1105.
- [10] R. Franz, J. Neidhardt, B. Sartory, R. Tessadri, C. Mitterer, *Thin Solid Films* 516 (2008) 6151–6157.
- [11] R. Franz, J. Neidhardt, C. Mitterer, B. Schaffer, H. Hutter, R. Kaindl, B. Sartory, R. Tessadri, M. Lechthaler, P. Polcik, *J. Vac. Sci. Technol. A* 26 (2008) 302–308.
- [12] R. Franz, J. Schnöller, H. Hutter, C. Mitterer, *Thin Solid Films* 519 (2011) 3974–3981.
- [13] K. Bobzin, N. Bagcivan, M. Ewering, R.H. Brugnara, S. Theiß, *Surf. Coat. Technol.* 205 (2011) 2887–2892.
- [14] Y.X. Xu, C. Hu, L. Chen, F. Pei, Y. Du, *Ceram. Int.* 44 (2018) 7013–7019.
- [15] W. Tillmann, D. Kokalj, D. Stangier, M. Paulus, C. Sternemann, M. Tolan, *Surf. Coat. Technol.* 328 (2017) 172–181.
- [16] H.C. Nguyen, Z. Joska, Z. Pokorný, Z. Studený, J. Sedlák, J. Majerík, E. Svoboda, D. Dobrocký, J. Procházka, Q.D. Tran, *Materials* 14 (2021).
- [17] W. Tillmann, D. Kokalj, D. Stangier, M. Paulus, C. Sternemann, M. Tolan, *Appl. Surf. Sci.* 427 (2018) 511–521.
- [18] H.C. Nguyen, Z. Joska, Z. Pokorný, Z. Studený, J. Sedlák, J. Majerík, E. Svoboda, D. Dobrocký, J. Procházka, Q.D. Tran, *Materials (Basel)* 14 (2021).
- [19] D. Klaffke, *Tribotest J.* 7 (2001) 281–299.
- [20] S. Iram, F. Cai, J. Wang, J. Zhang, J. Liang, F. Ahmad, S. Zhang, *Coatings* 10 (2020).
- [21] R. Wang, H. Mei, R. Li, T. Zhang, Q. Wang, *Surf. Coat. Technol.* 407 (2021).
- [22] A. Matsumura, *J. Vac. Sci. Technol. A* 21 (2003) S224–S231.
- [23] A.M. Korsunsky, M.R. McGurk, S.J. Bull, T.F. Page, *Surf. Coat. Technol.* 99 (1998) 171–183.
- [24] E.S. Puchi-Cabrera, J.A. Berrios, D.G. Teer, *Surf. Coat. Technol.* 157 (2002) 185–196.
- [25] J.J. Ayerdi, A. Aginagalde, I. Llavori, J. Bonse, D. Spaltmann, A. Zabala, *Wear* 470–471 (2021).
- [26] R. Kaindl, R. Franz, J. Soldan, A. Reiter, P. Polcik, C. Mitterer, B. Sartory, R. Tessadri, M. O'Sullivan, *Thin Solid Films* 515 (2006) 2197–2202.
- [27] Z. Li, P. Munroe, Z.-t. Jiang, X. Zhao, J. Xu, Z.-f. Zhou, J.-q. Jiang, F. Fang, Z.-h. Xie, *Acta Mater.* 60 (2012) 5735–5744.
- [28] A. Gilewicz, T. Kuznetsova, S. Aizikovitch, V. Lapitskaya, A. Khabarava, A. Nikolaev, B. Warcholinski, *Materials* 14 (2021).
- [29] R. Kaindl, B. Sartory, J. Neidhardt, R. Franz, A. Reiter, P. Polcik, R. Tessadri, C. Mitterer, *Anal. Bioanal. Chem.* 389 (2007) 1569–1576.
- [30] Z. Zhou, W.M. Rainforth, Q. Luo, P.E. Hovsepian, J.J. Ojeda, M.E. Romero-Gonzalez, *Acta Mater.* 58 (2010) 2912–2925.
- [31] K. Kutschej, P.H. Mayrhofer, M. Kathrein, P. Polcik, C. Mitterer, *Surf. Coat. Technol.* 200 (2005) 1731–1737.
- [32] F. Fernandes, J.C. Oliveira, A. Cavaleiro, *Surf. Coat. Technol.* 308 (2016) 256–263.
- [33] J. Restrepo, G. Mondragon-Rodriguez, J.M. Gonzalez-Carmona, J.M. Alvarado-Orozco, O. Garcia-Zarco, S.E. Rodil, J. Mater. Eng. Perform. (2021), <https://doi.org/10.1007/s11665-021-06333-8>.